Solar Energy 139 (2016) 381–388

Contents lists available at ScienceDirect

Solar Energy

journal homepage: www.elsevier.com/locate/solener

Shading-induced failure in thin-film photovoltaic modules: Electrothermal simulation with nonuniformities

M. Nardone *, S. Dahal, J.M. Waddle

Department of Physics and Astronomy, Bowling Green State University, Bowling Green, OH 43403, USA

ARTICLE INFO

Article history:
Received 15 July 2016
Received in revised form 3 October 2016
Accepted 6 October 2016

Keywords:
Numerical simulation
Reverse bias breakdown
Degradation
Monolithic modules
Cu(In,Ga) Se

ABSTRACT

Finite element electrothermal modeling is employed to study shading-induced failure in monolithically integrated thin-film photovoltaic modules. A key element is spatial nonuniformity in current-voltage characteristics, which causes inhomogeneous current flow when part of a module is under reverse bias due to shading. Time-dependent calculations show that spots with lower reverse breakdown voltage experience greater current density and localized thermal runaway that can cause permanent damage, resulting in ohmic shunts. Such failure events lead to performance loss, especially when the module is in normal operating conditions and shunted currents lead to abnormally high module temperatures. Our simulations of temperature distributions, current-voltage characteristics, and electroluminescence are compared to data from the literature for copper indium gallium diselenide devices.

© 2016 Elsevier Ltd. All rights reserved.

1. Introduction

Thin-film photovoltaic (PV) devices, such as amorphous silicon (a-Si), cadmium telluride (CdTe), and copper indium gallium diselenide (CIGS), have the distinct cost advantage of large area deposition. By laser scribing, those large areas are divided into individual series-connected cells to form monolithically integrated modules (Hegedus, 2006). A negative side-effect of that process is that nonuniformities are inevitable and can lead to transport and degradation mechanisms that are not as likely in crystalline PV devices (Karpov et al., 2002, 2004a). In addition, the use of bypass diodes to protect against shading-related power loss and degradation is challenging in monolithic modules (Dongaonkar et al., 2013; Lee et al., 2016). When a module is shaded within a series connected system of modules, bypass diodes can prevent the shaded module from experiencing reverse bias. If the bypass diodes open, the shaded module is effectively under short-circuit condition. If the bypass diodes should fail or be otherwise ineffective, the shaded module can experience reverse bias stress, which consumes energy from the other modules and is even more dangerous for the shaded module.

When an illuminated module is partially shaded, the darkened regions can experience reverse bias. It has been observed that CIGS modules subjected to reverse bias stress develop white, worm-like features visible under the glass that were associated with hot-spot ignition (Lee et al., 2016; Westin et al., 2009; Silverman et al., 2015a,b). Random ignition events were identified as correlated voltage and thermography pulses over the course of several minutes under dark, reverse-bias stress (Westin et al., 2009) and by electroluminescence (EL) within seconds during partial shading stress tests (Lee et al., 2016; Silverman et al., 2015a). The effects of such damage were increased shunt conductance and module power loss. The nature of shading-induced degradation in thin-film modules is an open and important problem (Kozinsky et al., 2016).

In this work, we investigate shading-induced failure in thin-film modules using electrothermal numerical simulation. We consider CIGS devices as a case study, but our approach is valid for other types of thin-film modules. Spatial and temporal variations of current and temperature are calculated to better understand the stresses caused by shading and the concomitant reverse bias. The typically observed (Szaniawski et al., 2013; Puttnins et al., 2014) reverse breakdown characteristic of CIGS devices is included in our model and we argue that the presence of low reverse breakdown voltage points (spatial nonuniformity) is a key factor in shading-induced failure. Our results demonstrate an example of thermal instability as a positive feedback mechanism in a nonuniform thin-film, the physics of which was described in Karpov (2012). In what follows, we distinguish between 'breakdown' and 'failure' by reserving 'breakdown' for the commonly observed increase in current with reverse voltage bias, and 'failure' for the localized, thermal runaway damaging event.

* Corresponding author.
E-mail address: marcon@bgsu.edu (M. Nardone).

http://dx.doi.org/10.1016/j.solener.2016.10.006
0038-092X/© 2016 Elsevier Ltd. All rights reserved.

Here we employ the Finite Element Method (FEM) using COMSOL Multiphysics® for quantitative electrothermal analysis of thin-film modules. Cell and module scale electrical simulations based on a network of equivalent circuits are commonly executed using a program such as SPICE (Brecl et al., 2005; Shvydka and Karpov, 2005; Brecl and Topi, 2008; Koishiyev, 2010; Pieters, 2011; Steiner et al., 2011). Electrothermal coupling can also be accomplished using such methods by translating the thermal problem into circuit elements (Maffezzoni and Amore, 2009; Vasko et al., 2014). With FEM, the partial differential equations are discretized by a customizable mesh and recent studies have shown that it can effectively simulate monolithic PV modules (Malm and Edoff, 2008; Lanz et al., 2013; Silverman et al., 2015b). Partial shading of thin-film modules was studied by equivalent circuit simulation for the case of uniform material properties (Dongaonkar et al., 2013). An advantage of the FEM approach is that irregularities in shape, material properties, and external conditions can be easily handled. Moreover, given that nonuniformity is a primary factor in our study, the ability of FEM to easily include localized variations with increased mesh refinement is essential.

2. Module simulation methodology

2.1. Electrical current

A schematic of one interconnect section of our monolithic module model is shown in Fig. 1 where the lateral current density, J, flows through the electrodes and is fed by the transverse current densities (lower case j's). The module model is based on the idea that each cell is comprised of electrical circuit elements connected in parallel to each other via a bottom electrode (back contact, metal) and top electrode [front contact, transparent conductive oxide (TCO)]. In the limit of infinitesimal spacing, current conservation requires that $\nabla \cdot J = Q_j$, where $Q_j = j/d$ is the current that enters per unit volume of electrode of thickness d. From Ohm's Law, $J = -\sigma\nabla\phi$, and the fact that we must consider current flow through both the front and back contacts, we obtain the coupled equations,

$$\nabla \cdot \left(-\sigma_f \nabla \phi_f\right) = -j/d_f, \tag{1}$$

$$\nabla \cdot \left(-\sigma_b \nabla \phi_b\right) = j/d_b, \tag{2}$$

where σ_f and σ_b are the conductivities of the front and back contacts, and $\phi_f(x,y)$ and $\phi_b(x,y)$ are the electric potential distributions. Conductivity can be obtained from the sheet resistance ($R_\square$ in units of $\Omega/\square$) by, $\sigma = 1/(R_\square d)$. The coupling is provided by the transverse current, j, because any current exiting the back contact must enter the front and vice versa.

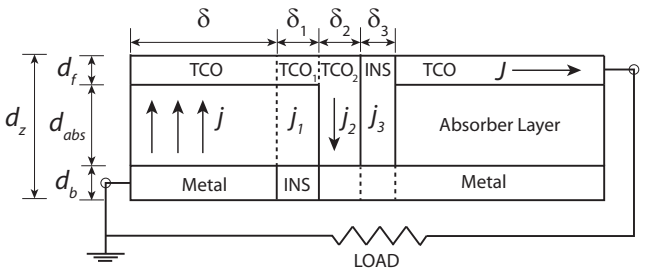

Fig. 1. Monolithic module schematic of one interconnect section. Dashed lines indicate current domains, not material breaks. INS is insulating material. Light is incident from the top. This schematic is a simplified representation of a typical substrate configuration device, such as commercial CIGS.

We assume that lateral current through the absorber can be neglected relative to that through the electrodes. This approach allows us to solve two coupled 2D models rather than one 3D model with a very large aspect ratio. As shown in Fig. 1, one end of the bottom contact is grounded while fixed voltage or current can be applied to the opposite end of the front contact. Given those boundary conditions, one can obtain current-voltage (IV) characteristics by integrating the current density over the boundary area (product of electrode length and d), which can be done for any contact shape.

Of the four transverse current domains indicated in Fig. 1, j is the diode current, $j_1 = j_3 = 0$, and $j_2 = (\phi_f - \phi_b)\sigma_2/h$ is an ohmic current through the vertical interconnect of conductivity σ_2 (we assume $\sigma_2 = \sigma_f$). The diode current is,

$$j = j_0 f_{rb}(V)\left[\exp\left(\frac{qV}{AkT}\right) - 1\right] - j_L, \tag{3}$$

where q is the elementary charge, $V = \phi_f - \phi_b$ is the local potential difference across the device, A is the ideality factor, k is Boltzmann's constant, and T is temperature. We use for the photocurrent $j_L = 32.5$ mA/cm^2 (typical for CIGS at 1-sun light). The function $f_{rb}(V)$ provides the observed reverse breakdown characteristics as described below [cf. Eq. (5)]. We estimate the saturation current as $j_0 = qGL$ where the G is the generation rate and L is the characteristic collection length of generated carriers. Given that the diffusion length, L_d, and depletion width, W_d, are of the same order ($L_d \approx W_d \approx 0.1$–$1$ μm) for CIGS, we use $L = 0.3$ μm. That also implies that most of the generation is within or close to the depletion region, hence $G = n_i/\tau$ in the dark, where n_i is the intrinsic concentration and τ is the minority carrier lifetime. With the standard expression for n_i the saturation current is given by,

$$j_0 = j_{00}\exp\left(-\frac{E_g}{2kT}\right) \quad \text{with} \quad j_{00} = \frac{qL\sqrt{N_c N_v}}{\tau}, \tag{4}$$

where E_g is the band gap, and N_c and N_v are the effective density of state in the conduction and valence bands. For our purposes, only exponential voltage and temperature dependencies are considered. The physical interpretation of Eq. (4) leads to an ideality factor of $A = 2$.

To minimize the number of tunable parameters, the above represents the simplest possible diode model that emphasizes the significant recombination/generation processes that occur in the depletion region of these thin-film heterostructures. A more detailed (e.g. two-diode) approach would include generation processes within the quasi-neutral bulk and an ideality factor between 1 and 2, which is typically observed. The presence of a high density of states at the CIGS/CdS interface and accounting for the observed $A > 2$ requires consideration of mechanisms that go beyond the two-diode model (Rau, 1999; Nardone et al., 2009). The simple model of Eq. (4) is suitable for the present scope of work but any diode model could be included within our electrothermal module simulation framework.

In this study, all of the parameters in Eq. (4) except for τ are fixed to reasonable values for CIGS (Gloeckler et al., 2003). The lifetime is varied to account for differences between normal and weak diodes (Karpov et al., 2002), as well as light and dark JV curves under forward bias. For example, Eq. (3) is plotted in Fig. 2 with lifetimes of $\tau = 10$ ns and $\tau = 5$ ns for a normal diode in the dark and in 1-sun light, respectively, and $\tau = 2$ ns for a weak diode in 1-sun light. As lifetime is decreased from 5 ns to 2 ns, V_{oc} declines from 0.61 V to 0.56 V and efficiency from 14.4% to 12.8%. That relationship between τ and V_{oc} is in agreement with experimental findings for CIGS devices (Repins et al., 2010). Overall, the forward bias JV curves are typical for CIGS, including the cross-over in light and dark curves at a voltage slightly greater than V_{oc}. Results from

Download English Version:

https://daneshyari.com/en/article/5451399

Download Persian Version:

https://daneshyari.com/article/5451399

Daneshyari.com